# STRIPLINES

## BASIC CONFIGURATION

The stripline, shown in Fig. 1, is the oldest planar transmission line and has been in use in microwave integrated circuits since its creation by R. M. Barrett in 1950 (1). In its simplest form, it consists of a conducting strip, of width $W$ and thickness $t$, separated from a pair of common conducting ground planes of theoretically infinite extent compared to the width $W$ of the strip conductor, $W \ll a$, where $a$ is the width of the ground plane. The ground planes are separated by a thickness $b$, and the entire space is homogeneously filled with a dielectric material of complex dielectric constant $\epsilon_r(1 - j \tan \delta)$. The ground planes are kept at the same potential. In a balanced stripline, the strip conductor is equidistant from the ground planes. In an unbalanced stripline, there is an offset

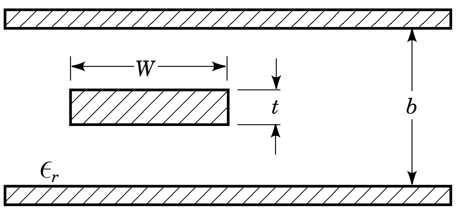


**Figure 1.** Balanced stripline configuration.

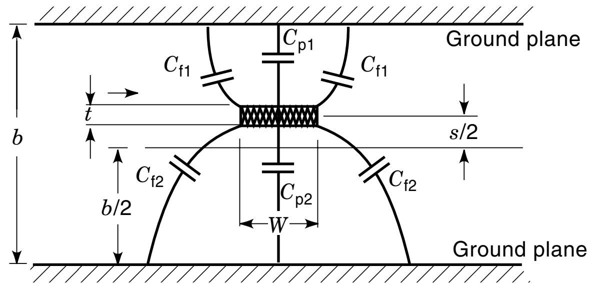


**Figure 2.** Unbalanced stripline configuration.

and the strip is not equidistant from the two ground planes, as shown in Fig. 2. The first significant theoretical investigation of striplines was carried out by S. Cohn in the mid-1950s (2). While Sanders Associates used the trade name *triplate* (3), the term *stripline* was first introduced by Airborne Instruments Laboratories (AIL).

## MODES IN A STRIPLINE AND THE MAXIMUM USABLE FREQUENCY

Although striplines can support waveguide-type modes (TE or TM), the fundamental mode of propagation is the transverse electromagnetic (TEM) mode, which has no cutoff frequency. The field configuration for the fundamental mode is shown in Fig. 3. The usable single-mode bandwidth of a stripline is determined by the cutoff frequency of the lowest-order waveguide mode. For that mode, the two ground planes have the same potential, the electric field is normal to the strip and the ground planes, and the longitudinal electric field is zero with a cutoff frequency (4)

$$f_c = \frac{c}{\sqrt{\epsilon_r}\left(2\frac{W}{b} + 4\frac{d}{b}\right)b} \tag{1}$$

where $c$ is the velocity of light in free space ($3 \times 10^8$ m/s) and $4b/d$ is a function of the cross section of the stripline. For a balanced stripline, when $t/b = 0$ and $W/b > 0.35$, then $4d/b$ is a function of $bc/f_c$, alone and is given in Table 1 (4).

## CHARACTERISTIC IMPEDANCE OF A BALANCED STRIPLINE

The characteristic impedance of a balanced strip transmission line can be accurately calculated from (5)

$$Z_0 = \frac{60}{\sqrt{\epsilon_r}} \ln\left[\frac{4b}{\pi d}\right] \tag{2}$$

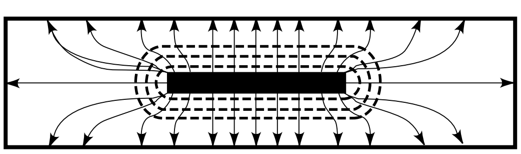


**Figure 3.** Field configuration of the fundamental mode of stripline.

**Table 1. The Quantity $4d/b$ versus $b/\lambda_c$ for $w/b \geq 0.35$ and $t/b \approx 0$**

| $b/\lambda_c$ | $4d/b$ |
|---|---|
| 0.00 | 0.882 |
| 0.20 | 0.917 |
| 0.30 | 0.968 |
| 0.35 | 1.016 |
| 0.40 | 1.070 |
| 0.45 | 1.180 |
| 0.50 | 1.586 |

For $W/b < 0.35$, where

$$d = \frac{W}{2}\left[1 + \frac{t}{\pi W}\left(1 + \ln\frac{4\pi W}{t} + 0.51\pi\left(\frac{t}{W}\right)^2\right)\right] \tag{3}$$

and

$$Z_0 = \frac{94.15}{\sqrt{\epsilon_r}} \frac{1}{\dfrac{C_f}{\epsilon} + \dfrac{W}{b\left(1 - \dfrac{t}{b}\right)}}\ \Omega \tag{4}$$

for $W/b \geq 0.35$ where

$$\frac{C_f}{\epsilon} = \frac{1}{\pi}\left\{\frac{2}{1 - \dfrac{t}{b}} \ln\left(\frac{1}{1 - \dfrac{t}{b}} + 1\right)\right\} - \frac{1}{\pi}\left\{\left(\frac{1}{1 - \dfrac{t}{b}} - 1\right) \ln\left(\frac{1}{\left(1 - \dfrac{t}{b}\right)^2} - 1\right)\right\} \tag{5}$$

$2C_f/\epsilon$ is the per-unit-length fringing field capacitance between the strip and each ground plane and $\epsilon = \epsilon_0\epsilon_r$; $\epsilon_0 = 8.854 \times 10^{-12}$ F/m (permittivity of free space).

## CHARACTERISTIC IMPEDANCE OF AN UNBALANCED STRIP TRANSMISSION LINE

The characteristic impedance of an unbalanced stripline (shown in Fig. 2) is given by (5)

$$Z_0 = \frac{120\pi}{\sqrt{\epsilon_r}\dfrac{C}{\epsilon}} \tag{6}$$

where $C/\epsilon$ is the per-unit-length static capacitance between the strip and the two ground planes, normalized by the permittivity $\epsilon$ of the medium.

$$\frac{C}{\epsilon} = \frac{C_{p1}}{\epsilon} + \frac{C_{p2}}{\epsilon} + \frac{2C_{f1}}{\epsilon} + \frac{2C_{f2}}{\epsilon} \tag{7}$$

$$\frac{C_{p1}}{\epsilon} = \frac{2\dfrac{W}{b - s}}{1 - \dfrac{t}{b - s}} \tag{8}$$

$$\frac{C_{p2}}{\epsilon} = \frac{2\dfrac{W}{b + s}}{1 - \dfrac{t}{b + s}} \tag{9}$$

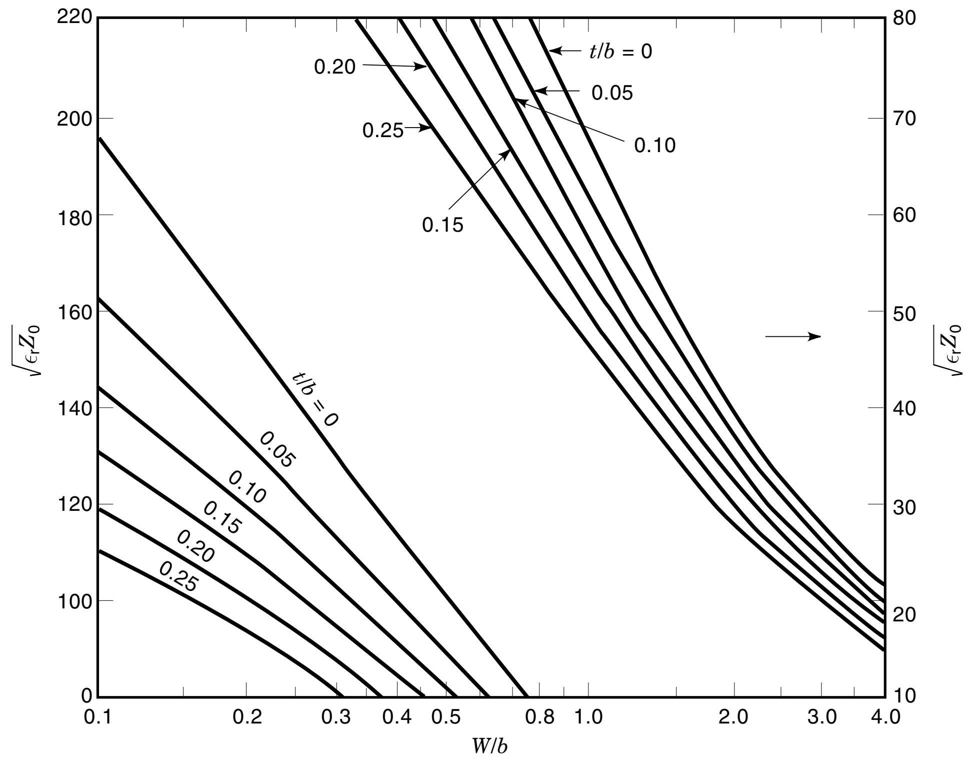


**Figure 4.** Variation of characteristic impedance $Z_0$ with $W/b$ and $t/b$.

The per-unit-length fringe field capacitances $C_{f1}$ and $C_{f2}$ are obtained from Eq. (5) by replacing $b$ with $(b - s)$ and $(b + s)$, respectively. The preceding formulas are applicable to single strips only. Figure 4 shows the variations of $Z_0$ with $W/b$ for various values of $t/b$, for a balanced stripline.

## THE PROPAGATION CONSTANT IN A STRIPLINE

The propagation constant $\beta$ of a stripline is given by

$$\beta = \frac{2\pi}{\lambda_g} = \frac{2\pi\sqrt{\epsilon_r}}{\lambda_0} \text{ rad/unit length} \tag{10}$$

where $\lambda_g$ and $\lambda_0$ are the wavelengths in the stripline and free space, respectively.

## SYNTHESIS OF STRIPLINES

To obtain the structural dimensions for a stripline to be designed, when the characteristic impedance $Z_0$ and the substrate dielectric constant $\epsilon_r$ are given, the following formula is used (6):

$$W = W_0 - \Delta W_0 \tag{11}$$

$$W_0 = \frac{8(b-t)\sqrt{B+0.568}}{\pi(B-1)} \tag{12}$$

$$\Delta W_0 = \frac{t}{\pi}\left\{1 - 0.5\ln\left[\left(\frac{t}{2b-t}\right)^2 + \left(\frac{0.0796t}{W_0 - 0.26t}\right)^m\right]\right\} \tag{13}$$

$$B = e^{\left(\frac{Z_0\sqrt{\epsilon_r}}{30}\right)} \tag{14}$$

and

$$m = 6\left[\frac{b-t}{3b-t}\right] \tag{15}$$

There is no closed-form design equation for the unbalanced stripline shown in Fig. 2. An iterative procedure based on analysis and optimization is used to synthesize an unbalanced stripline for a given characteristic impedance $Z_0$ and substrate dielectric constant $\epsilon_r$.

## ATTENUATION CONSTANT IN STRIPLINES

The attenuation constant of a stripline, balanced or unbalanced, is given by (4)

$$\alpha = \alpha_c + \alpha_d \text{ Np/unit length} \tag{16}$$

The attenuation constant $\alpha_c$ due to conductor loss in the line at a frequency $f$ in gigahertz is obtained from (7)

$$\alpha_c = \frac{\pi\sqrt{\epsilon_r}f}{0.2998}\left[1 - \frac{Z_0}{Z_0'}\right] \text{Np/m} \tag{17}$$

where $Z_0$ is the characteristic impedance of the line and $Z_0'$ is the characteristic impedance of the line when $W$, $t$, and $b$ are replaced by $W = W + \delta_s$, $t + \delta_s$, and $b - \delta_s$, respectively, in Eqs. (2) to (5).

$$\delta_s = 0.0822\sqrt{\frac{\rho_r}{f}} \text{ mil} \tag{18}$$

is the skin depth a the frequency $f$ in GHz. $\rho_r$ is the resistivity of the metal with respect to copper.

The attenuation constant $\alpha_d$ due to dielectric loss is given by

$$\alpha_d = \frac{\beta \tan\delta}{2} \text{ Np/m} \tag{19}$$

where tan $\delta$ is the loss tangent of the material. The $Q$-factor of a stripline is given by

$$Q = \frac{8.686\pi\sqrt{\epsilon_r}}{\lambda_0 \alpha} \tag{20}$$

## THE POWER-HANDLING CAPABILITY OF STRIPLINES

The average power $P$, in kW, that can be carried by a matched balanced stripline with rounded edges is shown in Fig. 5 (4). The ground plane to ground plane thickness is measured in inches. Although the strip edges are assumed to be round, an approximate value of $Z_0$ can be obtained from either Fig. 4 or from the analysis equations presented previously.

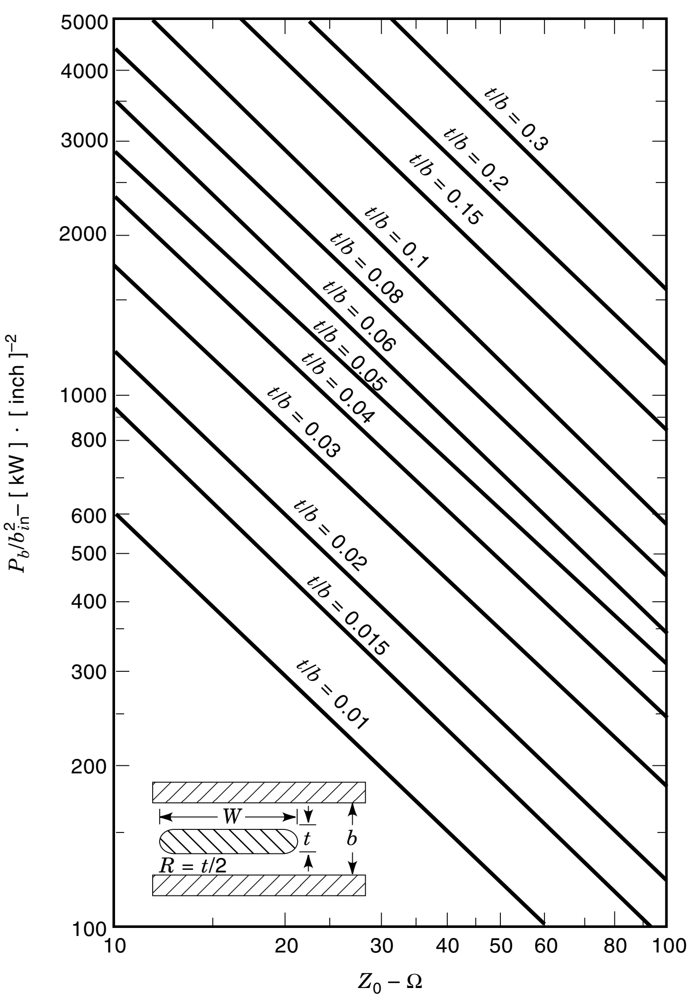


**Figure 5.** Average power handling capability of a stripline with rounded trip edges.

## STRIPLINE DISCONTINUITIES

Stripline discontinuities are as essential an element of microwave circuits as their uniform line counterpart. Any arbitrary discontinuity in a stripline can be decomposed into a few basic forms of discontinuities. These are an abrupt change in width or step discontinuity, a gap, a circular hole in the strip, an open end, a cross junction, a $T$-junction, and an angled bend. The appearance of discontinuities causes alterations in the electromagnetic field configurations of an otherwise uniform stripline. Therefore, the modified field configuration can be taken into account by appropriate incorporation of a shunt or a series capacitance or inductance. For example, an open end can be represented by a shunt capacitance. Figure 6 shows the configurations and the corresponding equivalent circuits of the discontinuities (8–10). The equivalent width $D$, shown by the dashed lines, is obtained by conformal mapping techniques:

$$D = b\frac{K(k)}{K(k')} + \frac{t}{\pi}\left(1 - \ln\frac{2t}{b}\right) \tag{21}$$

for $W/b \leq 0.35$ where $K(k)$ is the complete elliptic integral of the first kind

$$k = \tan h\left(\frac{\pi W}{2b}\right) \tag{22}$$

$$K(k) = \int_0^1 \frac{dx}{\sqrt{(1-x^2)(1-k^2x^2)}} \tag{23}$$

The associated complementary elliptic integral is defined as

$$K(k') = K(\sqrt{1-k^2}) \tag{24}$$

and

$$D = W + \frac{2b}{\pi}\ln 2 + \frac{t}{\pi}\left(1 - \ln\frac{2t}{b}\right) \tag{25}$$

for $W/b > 0.35$.

### Step Discontinuity

A change in strip width or step discontinuity is essential for the design of stripline matching transformers and low-pass filters. The equivalent circuit parameters, shown in Fig. 6(a), are given by

$$X = Z_1\frac{2D_1}{\lambda_g}\ln\csc\frac{\pi D_2}{D_1} \tag{26}$$

$$l_1 = -l_2 = \frac{b\ln 2}{\pi} \tag{27}$$

The normalized scattering matrix of the discontinuity can be written as

$$\begin{aligned}
[S] &= \frac{1}{\Delta}\begin{bmatrix} S_{11} & S_{12} \\ S_{21} & S_{22} \end{bmatrix} \\
S_{11} &= (Z_2 - Z_1 + jX)e^{-j2\beta l_1} \\
S_{12} &= S_{21} = 2\sqrt{Z_1 Z_2} \\
S_{22} &= (Z_1 - Z_2 + jX)e^{+j2\beta l_2} \\
\Delta &= Z_1 + Z_2 + jX
\end{aligned} \tag{28}$$

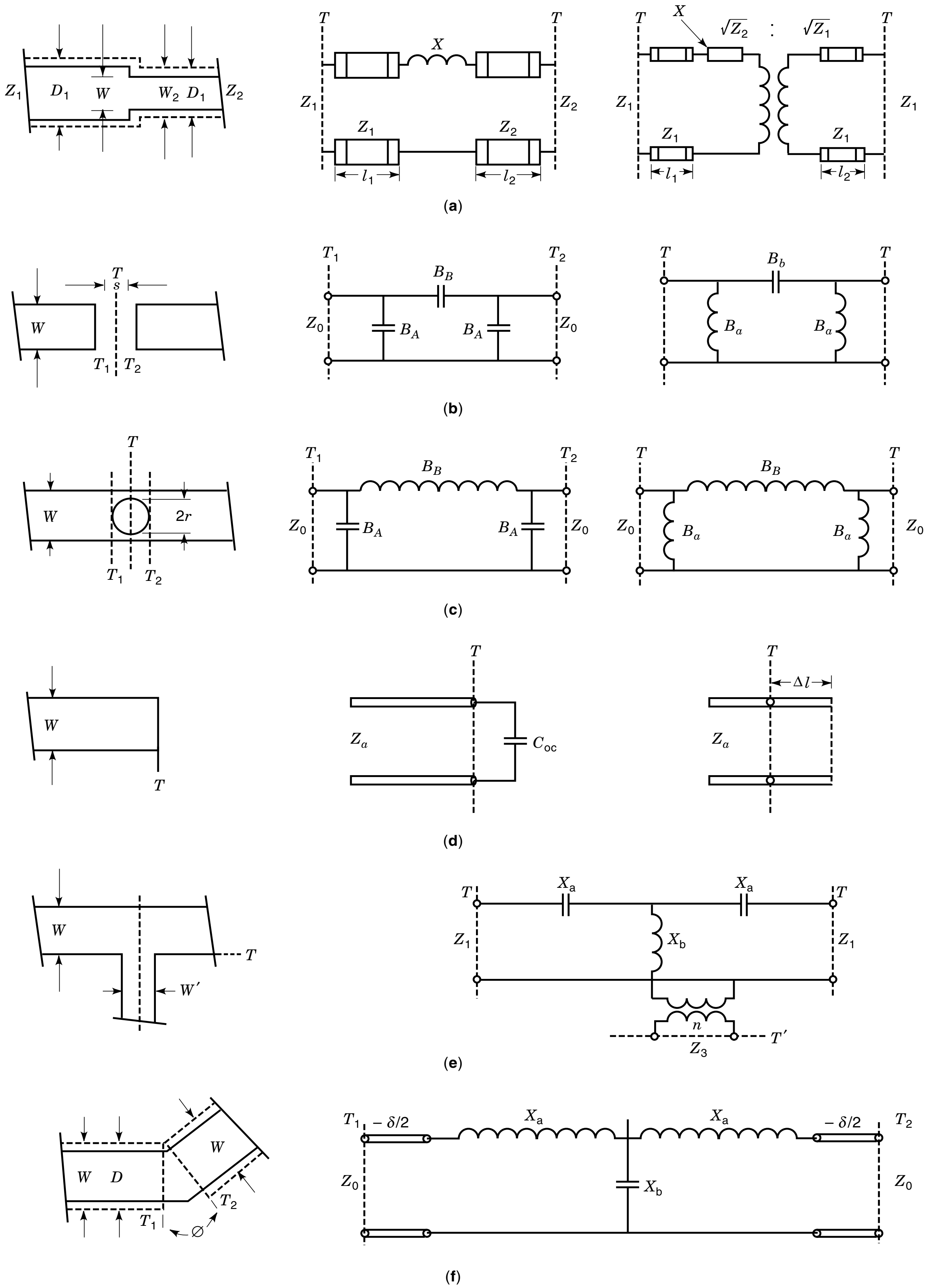


**Figure 6.** Stripline discontinuities and the equivalent networks: (a) step, (b) gap, (c) circular hole, (d) open end, (e) T-junction, (f) bend (10).

The equivalent network for equal normalizations at the input and the output ports includes a transformer, as shown in Fig. 6(a).

### Gap Discontinuity

A series capacitance in a stripline is realized by a gap discontinuity, as shown in Fig. 6(b). The equivalent circuit is, however, a pi-network of one series and two shunt capacitances. The series component is due to the fringing capacitance from one strip to the other strip, and the shunt components are due to the field disturbance at the edge of each strip. As the gap increases, the series capacitance decreases and the two shunt capacitances tend toward that of an open-ended stripline. The normalized susceptance parameters of the equivalent pi-network are given by

$$\overline{B_A} = \frac{1+\overline{B_a}\cot(\beta s/2)}{\cot(\beta s)-\overline{B_a}} = \frac{\omega C_1}{Y_0} \tag{29}$$

$$2\overline{B_B} = \frac{1+(2\overline{B_b}+\overline{B_a})\cot(\beta s/2)}{\cot(\beta s/2)-(2\overline{B_b}+\overline{B_a})} - \overline{B_A} = \frac{2\omega C_{12}}{Y_0} \tag{30}$$

$$\lambda\overline{B_a} = 2b\ln\left\{\operatorname{sech}\left(\frac{\pi s}{2b}\right)\right\} \tag{31}$$

$$\lambda\overline{B_b} = b\ln\left\{\coth\left(\frac{\pi s}{2b}\right)\right\} \tag{32}$$

### Circular Hole Discontinuity

A hole discontinuity in a stripline is introduced to realize reactive tuning in filters and resonators. Such discontinuities are predominantly inductive in nature. The most common hole discontinuity is a circular hole discontinuity, as shown in Fig. 6(c). The susceptance parameters of the equivalent pi-network are given by

$$\overline{B_A} = \frac{1+\overline{B_a}\cot(\beta r)}{\cot(\beta r)-\overline{B_b}} \tag{33}$$

$$2\overline{B_B} = \frac{1+2\overline{B_b}\cot(\beta r)}{\cot(\beta r)-\overline{B_b}} - \overline{B_A} \tag{34}$$

where

$$\overline{B_b} = -\left(\frac{3bD}{16\beta r^3}\right), \quad \overline{B_a} = \frac{1}{4\overline{B}_b} \tag{35}$$

The equivalent networks for gap and circular hole discontinuities depend on where the reference plane is considered to be situated.

### Open-End Discontinuity

An open-end discontinuity occurs whenever an open-circuited stripline stub is used in matching networks, filters, and so on. Figure 6(d) shows a stripline open end and two equivalent networks. The network can be a shunt capacitance $C_{oc}$ or an extended length $\Delta l$. The second representation assumes that a perfect magnetic wall exists at a distance $\Delta_l$ from the physical open circuit. The open-circuit capacitance is given by

$$C_{oc} = \frac{1}{\omega Z_0}\tan^{-1}\left[\frac{\xi+2W}{4\xi+2W}\tan(\beta\xi)\right] \tag{36}$$

where

$$\lambda = \frac{\lambda_0}{\sqrt{\epsilon_r}}, \quad \beta = \frac{2\pi}{\lambda}, \quad \xi = 0.2206b \tag{37}$$

The length extension $\Delta l$ can be obtained from the open-end capacitance

$$\Delta l = \frac{1}{\beta}\tan^{-1}(Z_0\omega C_{oc}) \tag{38}$$

The reflection coefficient from the open-end discontinuity can be calculated as

$$S_{11} = \frac{1-jZ_0\omega C_{oc}}{1+jZ_0\omega C_{oc}} \tag{39}$$

In the preceding equations, $Z_0$ is the characteristic equation of the stripline.

### T-Junction Discontinuity

A T-junction discontinuity occurs in stripline stub matching, stub-loaded lowpass and bandpass filters, branchline couplers, hybrid rings, and in many other components. Figure 6(e) shows the stripline T-junction and the equivalent network. The network parameters are obtained from

$$\frac{X_a}{Z_1} = -(0.785n)^2\frac{D_3^2}{D_1\lambda} \tag{40}$$

$$\frac{X_b}{Z_1} = -\frac{X_a}{2Z_1} + \frac{1}{n^2}\left\{\frac{B_1}{2Y_1} + \frac{2D_1}{\lambda}\left[0.6931 + \frac{\pi D_3}{6D_1} + 1.5\left(\frac{D_1}{\lambda}\right)^2\right]\right\} \tag{41}$$

for $D_3/D_1 < 0.5$, and

$$\frac{X_b}{Z_1} = -\frac{X_a}{2Z_1} + \frac{2D_1}{\lambda n^2}\left\{\ln\frac{1.43D_1}{D_3} + 2\left(\frac{D_1}{\lambda}\right)^2\right\} \tag{42}$$

for $D_3/D_1 > 0.5$. The transformer turns ratio $n$ is given by

$$n = \frac{\sin\left(\dfrac{\pi D_3}{\lambda}\right)}{\dfrac{\pi D_3}{\lambda}} \tag{43}$$

and

$$\frac{B_1}{2Y_1} = \frac{2D_1}{\lambda}\left[\ln\csc\frac{\pi D_3}{2D_1} + 0.5\left(\frac{d_1}{\lambda}\right)^2\cos^4\frac{\pi D_3}{2D_1}\right] \tag{44}$$

In the preceding equations $D_1$ and $D_3$ are the widths of the equivalent parallel plate waveguides for strips of widths $W$ and $W'$, respectively; $Z_1$ and $Z_3$ are corresponding characteristic impedances; and $Y_1$ and $Y_3$ are the respective characteristic admittances. The normalized scattering matrix of the T-junction is obtained from

$$S_{11} = S_{22} = \frac{j2(Z_3/n^2)X_a - (Z_1^2 + 2X_aX_b + X_a^2)}{(Z_1 + jX_a)\Delta} \quad (45)$$

$$S_{12} = S_{21} = \frac{2Z_1(Z_3/n^2 + jX_b)}{(Z_1 + jX_a)\Delta} \quad (46)$$

$$S_{13} = S_{23} = S_{31} = S_{32} = \frac{2\sqrt{Z_1Z_3}/n^2}{\Delta} \quad (47)$$

$$S_{33} = \frac{Z_1 - 2(Z_3/n^2) + j(X_a + 2X_b)}{\Delta} \quad (48)$$

and

$$\Delta = Z_1 + 2Z_3/n^2 + j(X_a + 2X_b) \quad (49)$$

### Bend Discontinuity

A bend discontinuity occurs mainly in stripline transitions and hybrids. Figure 6(f) shows a stripline bend discontinuity and the equivalent network. The parameters of the network are obtained from the following equations, derived from Babinet's principle and the equivalent parallel plate waveguide model.

$$\lambda\overline{X_a} = 2D\left\{\Psi(x) + 1.9635 - \frac{1}{x}\right\} \quad (50)$$

$$\overline{X_b} = -\frac{\lambda}{2\pi D}\cot\frac{\theta}{2} \quad (51)$$

With $\theta$, in degrees, $x$ is given by

$$x = 0.5\left\{1 + \frac{\theta}{180}\right\} \quad (52)$$

and

$$\Psi(x) = 0.5223\ln(x) + 0.394 \quad (53)$$

Equation (53) is an approximation of the T-function (11). Accurate values of the T-function for various x are available in Ref. 11.

The reference planes $T_1$ and $T_2$ meet at an angle $\theta$. This modifies the scattering parameters of the bend by multiplying $S_{11}$ and $S_{22}$ by $e^{j2\beta\zeta}$ and $S_{12}$ and $S_{21}$ by $e^{j\beta\zeta}$, where

$$\delta = (D - W)\tan\frac{\theta}{2} \quad (54)$$

## SUSPENDED STRIPLINE

Microstrip, the second-generation strip transmission line, became popular with the availability of low-loss and inexpensive dielectric, ferrite, and semiconducting substrates in the late 1960s (12). It is a derivative of stripline in which the top ground plane is theoretically moved to infinity and the space above the strip is filled with an air dielectric ($\epsilon_r = 1$), as shown in Fig. 7(a). Microstrip is the basic building block in microwave integrated circuit (MIC) and microwave monolithic integrated circuit (MMIC) technology (23).

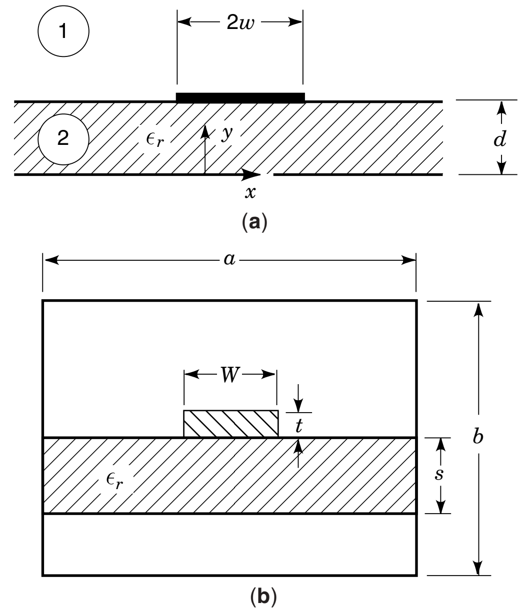


**Figure 7.** (a) Conventional unshielded microstrip line. (b) Suspended stripline.

Conventional microstrip, despite all its advantages at microwave frequencies, tends to be excessively lossy at millimeter-wave frequencies. Moreover, fabrication difficulties arise due the required small dimensional tolerances at these higher frequencies. To overcome these problems the suspended stripline configuration [Fig. 7(b)] was proposed (12). Suspended stripline incorporates air gaps between the substrate and the two ground planes, as shown in the generalized stripline in Fig. 8 (14) ($\epsilon_{r1} = \epsilon_{r3} = \epsilon_{r4} = 1$ and $\epsilon_{r2} = \epsilon_r$). This results in a low zero frequency effective dielectric constant $\epsilon_e(0)$ of the propagating medium (12). For suspended stripline the effective dielectric constant lies between the substrate dielectric constant $\epsilon_r$ and 1. Because of the low dielectric constant, the suspended stripline results in larger circuit dimen-

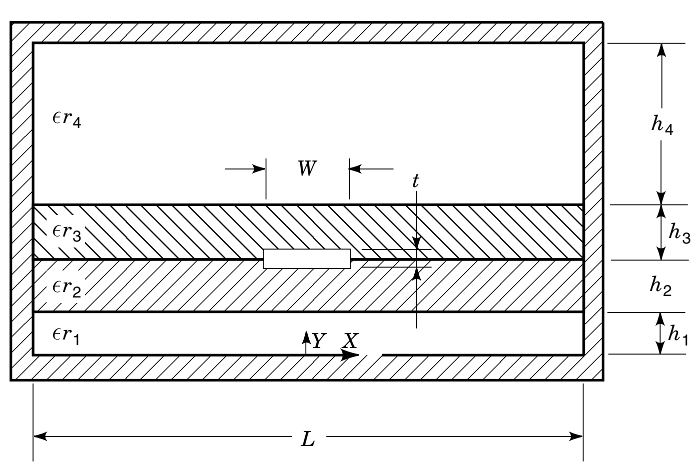


**Figure 8.** Generalized suspended stripline.

sions, leading to less stringent mechanical tolerances and increased fabricational accuracy. Moreover, incorporation of air gaps near the ground planes causes less field to be present near the ground plane and consequently reduces the conductor loss (12).

It is accepted that 110 GHz is the approximate upper frequency limit for operation of suspended stripline in millimeter-wave integrated circuits. This limitation results from the combination of techniques required for meeting fabricational tolerances and handling fragility and mode suppression. Losses in suspended stripline at higher frequencies become significant.

The growing density of millimeter-wave circuits and advantages offered by suspended stripline in terms of cross-sectional dimensions, frequency range of operation, leakage field confinement, and low-cost circuit design and development have resulted in the realization of many important circuit components in suspended stripline.

## ANALYSIS OF SUSPENDED STRIPLINE

### Quasistatic Analysis

Quasistatic analysis is restricted to the low-frequency region only; it evaluates the transmission characteristics from two capacitances: One is $C_a$, for a unit length of the stripline-like configuration obtained from Fig. 8 (13) with $\epsilon_{r1} = \epsilon_{r3} = \epsilon_{r4} = \epsilon_{r2} = \epsilon_r = 1$; and the other capacitance $C$ for a unit length of the suspended stripline $\epsilon_{r1} = \epsilon_{r3} = \epsilon_{r4} = 1$ and $\epsilon_{r2} = \epsilon_r$. The characteristic impedance $Z$ and the propagation constant $\beta$ of the line can written in terms of these two capacitances as

$$Z = \frac{1}{c\sqrt{CC_a}} \tag{55}$$

$$\beta = k_0\sqrt{\epsilon_e(0)} \tag{56}$$

$$\epsilon(0) = \frac{C}{C_a} \tag{57}$$

where $\epsilon_e(0)$ is the effective dielectric constant of the medium, $\beta = 2\pi/\lambda_g$, and $k_0 = 2\pi/\lambda_0$; $\lambda_g$ and $\lambda_0$ are the guided and the free space wavelengths, respectively; and c is the speed of electromagnetic waves in free space.

Consider Fig. 8 (13). This structure can be thought of as a special case of the multidielectric layer structure shown in Fig. 9(a). Let us assume that there is a point source at point ($x_0$, $y_0$). Green's function for this structure satisfies Poisson's equation as

$$\nabla_t^2 G(x, y|x_0, y_0) = -\frac{1}{\epsilon}\delta(x - x_0)\delta(y - y_0) \tag{58}$$

The following boundary conditions can be applied to Fig. 9(b), for continuity of fields at the $j$th interface of dielectrics

$$G(x, s_{j-0}) = G(x, s_{j+0}) \tag{59}$$

and

$$\epsilon_j \frac{\partial}{\partial y}[G(x, s_{j-0})] = \epsilon_{j+1}\frac{\partial}{\partial y}[G(x, s_{j+0})] \tag{60}$$

For a lossless, nonmagnetic and isotropic substrate material, the solution of Eq. (58) has the form

$$G = \sum_{n=1}^{\infty} G_n^x(x)G_n^y(y) \tag{61}$$

If we assume that the side walls at $x = 0$ and $x = L$ are perfect electric walls, then we can write

$$G_n^x(x) = \sin\left(\frac{n\pi x}{L}\right) \qquad n = 1, 2, 3\ldots\infty \tag{62}$$

Using Eq. (62) for $G_n^x(x)$ and substituting Eq. (62) in Eq. (58) gives

$$\sum_{n=1}^{\infty}\left\{\frac{d^2}{dy^2} - \left(\frac{n\pi}{L}\right)^2\right\} G_n^y(y)\sin\left(\frac{n\pi x}{L}\right) = -\frac{1}{\epsilon}\delta(x - x_0)\delta(y - y_0) \tag{63}$$

Multiplying both sides by $\sin(n\pi x/L)$ and integrating over period $x = 0$ to $x = L$ gives the differential equation for $G_n^y(y)$:

$$\left(\frac{d^2}{dy^2} - \beta_n^2\right) G_n^y(y) = -\frac{2}{L\epsilon}\sin(\beta_n x_0)\delta(x - X_0) \tag{64}$$

where $\epsilon$ is the permittivity of the region and $\beta_n = n\pi/L$. The preceding equation can be shown to be analogous to the differential equation with the parameters given by Ref. 14.

The characteristic admittance is

$$Y_0 = \epsilon \tag{65}$$

the propagation constant is

$$\gamma = \beta_n \tag{66}$$

and the voltage is

$$V = G_n^y(y) \tag{67}$$

Obviously, the solution to Eq. (63) is, therefore, given by

$$G_n^y(y) = \frac{2}{n\pi x}\sin(\beta_n x_0) \tag{68}$$

Combining Eqs. (61), (62), and (68) gives the solution for the Green's function at the charge plane at $y = y_0$ as

$$G(x, y_0|x_0, y_0) = \sum_{n=1}^{\infty}\frac{2}{n\pi\overline{\epsilon}}\sin(\beta_n x_0)\sin(\beta_n x) \tag{69}$$

where

$$\overline{\epsilon} = \epsilon_1 + \epsilon_2 \tag{70}$$

and

$$\epsilon_1 = \epsilon_{r2}\frac{\epsilon_{r1}\coth(\beta_n h_1) + \epsilon_{r2}\tanh(\beta_n h_2)}{\epsilon_{r2} + \epsilon_{r1}\coth(\beta_n h_1)\tanh(\beta_n h_2)} \tag{71}$$

$$\epsilon_{r2} = \epsilon_{r3}\frac{\epsilon_{r4}\coth(\beta_n h_3) + \epsilon_{r3}\tanh(\beta_n h_4)}{\epsilon_{r3} + \epsilon_{r4}\coth(\beta_n h_4)\tanh(\beta_n h_3)} \tag{72}$$

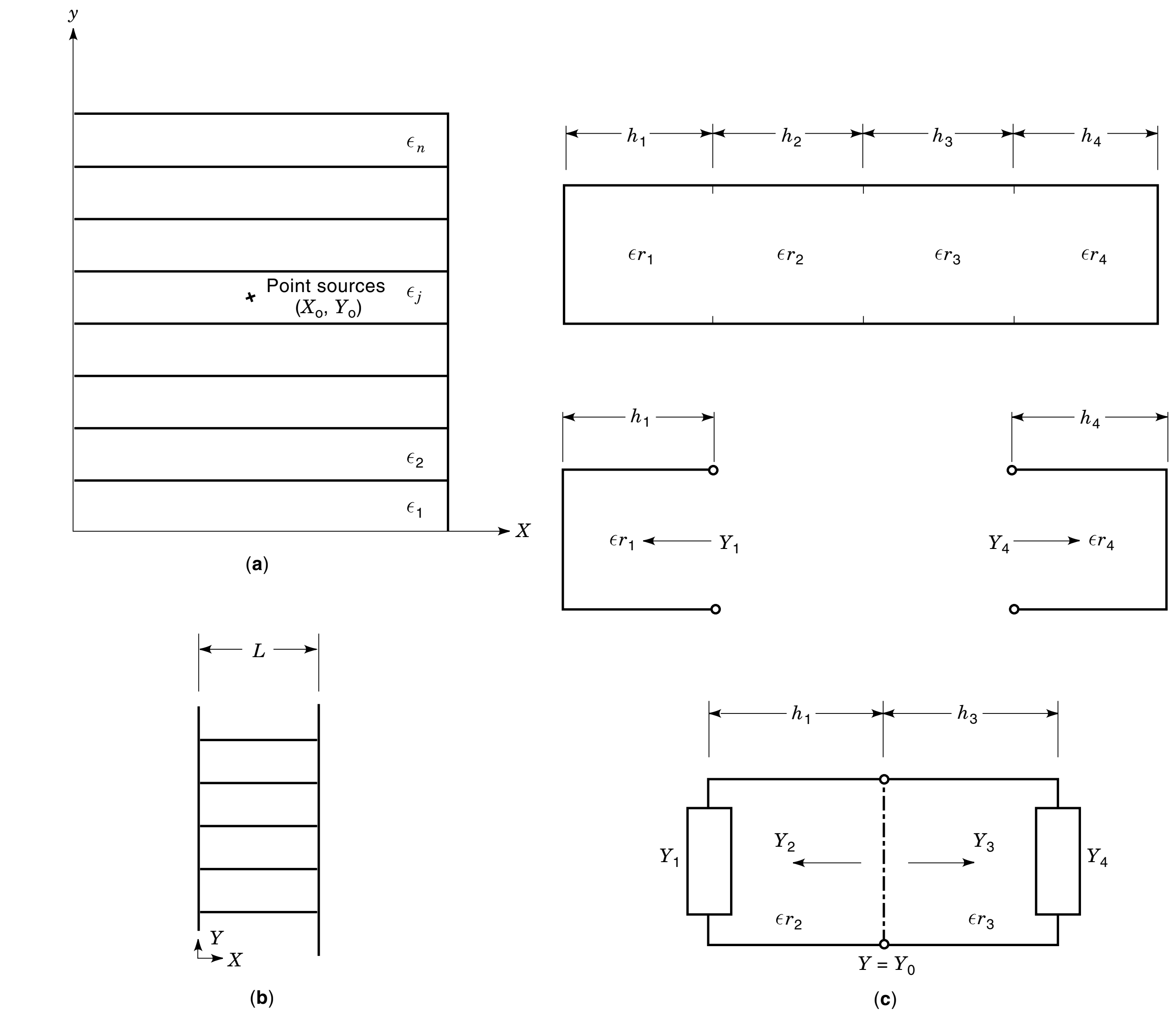


**Figure 9.** (a) Multilayered dielectric structure. (b) Representative structure for imposition of boundary condition. (c) The equivalent transmission line model.

The equivalent transmission line model is shown in Fig. 9(c). Knowing the Green's function, the line capacitance of the structure is evaluated using the variational expression (15)

$$C = \frac{\int_{s1} f(x)\,dx}{\int_{s1}\int_{s1} G(x, y_0|x_0, y_0) f(x) f(x_0)\,dx} \tag{73}$$

A wise choice of the trial function for the charge distribution $f(x)$ on the strip may give a very accurate value of $C$. Otherwise the most appropriate charge distribution is assumed to be

$$f(x) = \left(\frac{1}{W}\right)\left\{1 + K'\left|\frac{2}{W}\left(x - \frac{L}{2}\right)\right|^3\right\}; \quad \text{for} \quad \frac{L-W}{2} \le x \le \frac{L+W}{2} \tag{74}$$

The constant $K'$ is obtained by maximizing the capacitance $C$ (15) as

$$K' = -\frac{\sum_{n\,\text{odd}} [L_n P_n (L_n - 4M_n)]/(\overline{\epsilon})}{\sum_{n\,\text{odd}} [M_n P_n (L_n - 4M_n)]/(\overline{\epsilon})} \tag{75}$$

where

$$L_n = \sin\left(\frac{\beta_n W}{2}\right) \tag{76}$$

$$M_n = \left(\frac{2}{\beta_n W}\right)^3 \left\{3\left[\left(\frac{\beta_n W}{2}\right)^2 - 2\right]\cos\left(\frac{\beta_n}{2}\right) + \left(\frac{\beta_n W}{2}\right)\left[\left(\frac{\beta_n W}{2}\right)^2 - 6\right]\sin\left(\frac{\beta_n}{2}\right) + 6\right\} \tag{77}$$

$$P_n = \left(\frac{2}{n\pi}\right)\left(\frac{2}{\beta_n W}\right)^2 \tag{78}$$

Substitution of the preceding equations in Eq. (73) yields

$$C = \frac{(1 + 0.25K')^2}{\sum_{n \text{ odd}} \frac{T_n P_n}{\overline{\epsilon}}} \tag{79}$$

where

$$T_n = (L_n + K' M_n)^2 \tag{80}$$

To obtain $C$ and $C_a$, the preceding steps are repeated for $\epsilon_{r2} = \epsilon_r$ and $\epsilon_{r2} = 1$, respectively. Once $C$ and $C_a$ are obtained, the characteristic impedance $Z$ and the effective dielectric constant $\epsilon_r$ are calculated using Eqs. (55) and (57), respectively.

### Wave Theory Analysis

There are many methods for calculating the quasistatic parameters $Z$ and $\epsilon_e(0)$ of a suspended stripline. For a detailed account of analysis methods for suspended stripline and other related structures, the reader should refer to Ref. 16. Suspended stripline structure, however, being inhomogeneous, cannot support pure TEM modes. It can be shown that coupled LSE (longitudinal-section electric) and LSM (longitudinal-section magnetic) modes or a hybrid mode are supported by suspended stripline. As a result, the characteristic impedance and the effective dielectric constant of suspended stripline are not frequency independent. The dispersive nature of these parameters depends to a large extent on the value of $\epsilon_r$ and the thickness $h_2$ of the substrate. However, the most commonly used substrates have a dielectric constant lower than 3.8 so that the dispersion is minimized.

Several methods have been developed to calculate the dispersive properties of suspended stripline (16). Considering the availability of cheaper computing power than ever before, the finite element method (FEM) appears to be the most robust method for analysis of suspended stripline dispersion. In the finite element method, the cross section of the suspended stripline is divided into a number of triangular subregions. At the vertices of each triangular region, the Hertz potential is expressed in terms of the so-called shape functions and the integral that represents the total energy of the system. On minimization of this integral, the values of the potentials at the nodes are uniquely obtained and the field distribution in the structure is determined. The minimization function can be reduced to a set of linear equations of the form (17)

$$[A(\beta)][u] = \gamma(\beta)[B(\beta)][u] \tag{81}$$

The elements of the matrices $[A]$ and $[B]$ together with the eigenvalues $\gamma(\beta)$ are the functions of the propagation constant $\beta$. Commercially available two-dimensional partial differential equation solvers (18), based on the finite element method, can be used to solve dispersion problems in suspended stripline. Figure 10 shows the frequency dependence of various propagation constants of a suspended stripline (19).

### Losses in Suspended Stripline

Attenuation in a suspended stripline can be divided into two parts. The total attenuation is given by

$$\alpha = \alpha_c + \alpha_d \quad \text{Np/unit length} \tag{82}$$

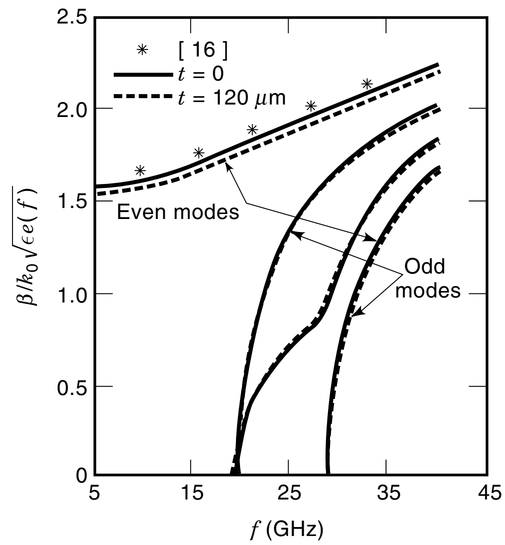


**Figure 10.** Frequency dependence of various propagation constants of a suspended stripline (19).

The attenuation $\alpha_c$, due to the conductor loss alone, is given by (12)

$$\alpha_c = \frac{0.072\lambda_g\sqrt{f}}{WZ_0}\left\{1 + \frac{2}{\pi}\tan^{-1}\left[1.4\left(\frac{\Delta}{\delta_s}\right)^2\right]\right\}\frac{\text{dB}}{\text{wavelength}} \tag{83}$$

where $f$ is the frequency in gigahertz, $Z_0$ is the characteristic impedance in ohms, $\Delta$ is the rms surface roughness, and $\delta_s$ is the skin depth at frequency $f$.

The attenuation constant $\alpha_d$ due to dielectric loss is given by (12)

$$\alpha_d = \frac{27.3\epsilon_r[\epsilon_e(0) - 1]\tan\delta}{\epsilon_e(0)(\epsilon_r - 1)}\frac{\text{dB}}{\text{wavelength}} \tag{84}$$

where tan $\delta$ is the loss tangent of the dielectric substrate. For all practical microwave applications of suspended stripline, it is observed that the conductor loss greatly exceeds the dielectric loss. Therefore, the attenuation constant due to dielectric loss can be neglected for all practical purposes.

## SUSPENDED STRIPLINE DISCONTINUITIES

As in conventional striplines, junctions or discontinuities are introduced in suspended striplines so that appropriate circuit

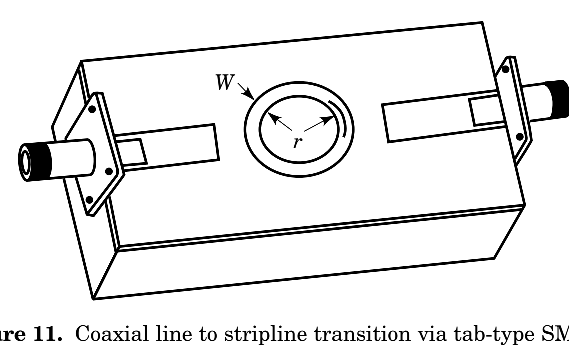


**Figure 11.** Coaxial line to stripline transition via tab-type SMA connector.

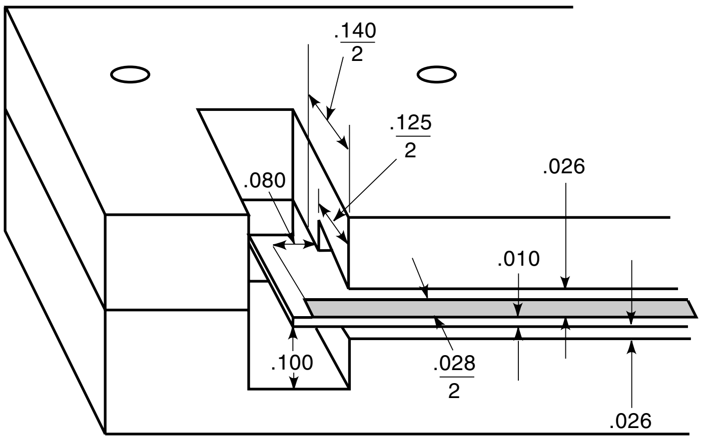


**Figure 12.** Millimeter-wave waveguide to suspended stripline transition.

functions may be performed. Typical discontinuities are the same as those of stripline and are shown in Fig. 6. In principle, all such discontinuities can be analyzed by extending the parallel plate waveguide approach used for the analysis of discontinuities in a balanced stripline. However, between 1980 and 1990 many researchers have analyzed suspended stripline discontinuities on the quasistatic and full-wave basis. A good account of this subject is available in Ref. 16. Currently, a number of those methods have been integrated into full-wave electromagnetic modeling based circuit analysis software packages, which are commercially available (20–22).

## STRIPLINE AND SUSPENDED STRIPLINE TRANSITIONS

Stripline is mainly used in the 0.5 GHz to 10 GHz range. Most transitions to stripline from other types of transmission line are achieved via a coaxial line and a tab-type SMA connector. Figure 11 shows a transition from a coaxial line to a stripline ring resonator (top substrate removed). Such transitions can offer good matching over a wide bandwidth. Matching as good as −35 dB can be achieved using these end launchers.

Suspended stripline is mainly used in the millimeter-wave band. Design of SMA tab-type end launchers with acceptable match is a difficult task. As a result, most transitions to suspended stripline are from millimeter-wave rectangular waveguide to suspended substrate stripline. Figure 12 shows a half-section probe transition from a rectangular waveguide to a suspended stripline (16). This type of junction can be accurately analyzed using three-dimensional electromagnetic solvers like HFSS from Hewlett Packard (20). Until now, not much work has been done on the analysis of transitions from suspended stripline to other millimeter-wave transmission lines.

## BIBLIOGRAPHY


1. R. M. Barrett, Microwave printed circuits—The early years, *IEEE Trans. Microw. Theory Tech.,* **MTT-32**: 983–900, 1984.
2. S. B. Cohn, Characteristic impedance of shielded strip transmission lines, *IRE Trans. Microw. Theory Tech.,* **MTT-2**: 52–55, 1954.
3. R. W. Peters et al., *Handbook of Triplate Microwave Components,* Sanders Associates, 1956.
4. G. Matthaei, L. Young, and E. M. T. Jones, *Microwave Filters, Impedance Matching Networks and Coupling Structures,* Norwood, MA: Artech House, 1974.
5. H. Howe, Jr., *Stripline Circuit Design,* Norwood, MA: Artech House, 1974.
6. H. A. Wheeler, Transmission line properties of a stripline between parallel planes, *IEEE Trans. Microw. Theory Tech.,* **MTT-26**: 866–876, 1978.
7. S. M. Perlow, Analysis of edge coupled shielded strip and slabline structures, *IEEE Trans. Microw. Theory Tech.,* **MTT-35**: 522–529, 1987.
8. A. A. Oliner, Equivalent circuits for discontinuities in balanced strip transmission line, *IRE Trans. Microw. Theory Tech.,* **MTT-3**: 134–143, 1955.
9. H. M. Altschuler and A. A. Oliner, Discontinuities in the center conductor of a strip transmission line, *IRE Trans. Microw. Theory Tech.,* **MTT-8**: 328–339, 1960.
10. K. C. Gupta, R. Garg, and R. Chadha, *Computer Aided Design of Microwave Circuits,* Norwood, MA: Artech House, 1981.
11. E. Jhanke and F. Emde, *Table of Functions,* New York: Dover, 1945, p. 16.
12. M. Schneider, *Bell Syst. Tech. J.,* **48**: 1421–1444, 1969.
13. P. Bhartia and I. J. Bahl, *Millimeter-Wave Engineering and Applications,* New York: Wiley, 1984.
14. B. Bhat and S. Koul, Unified approach to solve a class of strip and microstrip like transmission lines, *IEEE Trans. Microw. Theory Tech.,* **MTT-30**: 679–686, 1982.
15. R. E. Collin, *Field Theory of Guided Waves,* Piscataway, NJ: IEEE Press, 1995.
16. P. Pramanick and P. Bhartia, Microwave transmission lines, in T. K. Ishii (ed.), *Handbook of Microwaves,* New York: Academic Press, 1995.
17. J. Jin, *The Finite Element Method in Electromagnetics,* New York: Wiley, 1994.
18. PDEASE, *A Two Dimensional Partial Differential Equation Solver Based on the Finite Element Method,* Arlington, MA: Macsyma Inc., 1997.
19. R. Mansour, Ph.D. thesis, Dept. Electr. Eng., Univ. Waterloo, Waterloo, Ontario, Canada, 1987.
20. HFSS, High Frequency Circuit Solver, Palo Alto, CA: Hewlett-Packard, 1997.
21. Micro-stripes, 3-D Electromagnetic Solver, Nottingham, UK: Kimberly Communications Consultants, 1997.
22. SONNET, High Frequency Electromagnetic Software, Liverpool, NY: Sonnet Software Inc., 1997.
23. K. C. Gupta et al., *Microstrip Lines and Slotlines,* 2nd ed., Norwood, MA: Artech House, 1996.


PRAKASH BHARTIA
PROTAP PRAMANICK

**STRUCTURED PROGRAMMING.** See OBJECT-ORIENTED PROGRAMMING TRANSITION.

**STRUCTURE, MAGNETIC.** See MAGNETIC STRUCTURE.

**STRUCTURE OF INFORMATION RESOURCES.** See INFORMATION RETRIEVAL AND PUBLISHING.

**SUBMARINE CABLES.** See TELEGRAPHY, SUBMARINE.